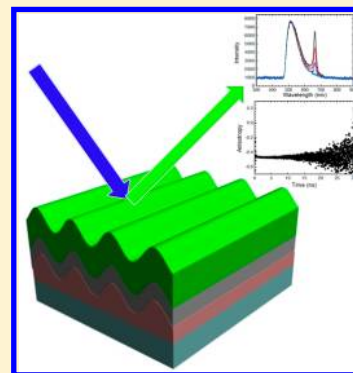


Time-Resolved Fluorescence Anisotropy of Surface Plasmon Coupled Emission on Metallic Gratings

Ya-Wei Hao,[†] Hai-Yu Wang,^{*,†} Zhen-Yu Zhang,[†] Xu-Lin Zhang,[†] Qi-Dai Chen,[†] and Hong-Bo Sun^{*,†,‡}[†]State Key Laboratory on Integrated Optoelectronics, College of Electronic Science and Engineering, Jilin University, 2699 Qianjin Street, Changchun 130012, China[‡]College of Physics, Jilin University, 2699 Qianjin Street, Changchun 130012, China

Supporting Information

ABSTRACT: The unique characteristics of surface plasmon coupled emission (SPCE) made it useful for potential applications in the fields of plasmonic optics and biological sensing. However, the mechanism of SPCE is still under debate. We studied the time-resolved fluorescence anisotropy of SPCE excluding the interference of absorption-enhancement effect by the time-correlated single-photon counting (TCSPC) setups. The value of anisotropy at SPCE peak kept constant at -0.45 during the whole relaxation process, which is in agreement with the calculated value. Our work presented a further step toward the understanding of SPCE.



INTRODUCTION

Surface plasmon polaritons (SPPs) are electromagnetic waves coupled to collective oscillation of free electrons propagating along the interface between a conductor and a dielectric.^{1,2} The electromagnetic field associated with SPPs is confined in the perpendicular direction to the interface and maximum at the interface as well as decaying exponentially. The confinement is achieved when the propagation constant is greater than the wave vector of the light in the dielectric, so the SPPs dispersion curve lies to the right of the light line. Therefore, SPPs could not be excited directly on a smooth metallic surface unless special techniques for phase-matching are employed. There are several experimental methods to overcome the mismatch for SPPs excitation, including prism coupling, grating coupling, waveguide coupling, and near-field excitation.^{1,3} The evanescent characteristic of SPPs shows a lot of unique properties such as strong electromagnetic field, transmission enhancement, and high sensitivity to the dielectric difference of adjacent environment. These properties make SPPs of renewed interest for potential applications in the fields of photovoltaic devices,^{4–7} light-emitting diodes,^{8–10} Raman spectroscopy,^{11–13} and enhanced fluorescence emission.^{14–19}

Among these potential applications, enhanced fluorescence emission based on SPPs has attracted a great deal of attention in recent years because of high improvement on the efficiency of OLED devices^{9,10} and extraordinary increase in the fluorescence sensitivity of biosensors.^{20–24} In the published works,^{15,25} researchers assigned the enhanced fluorescence emission to two possible mechanisms. One is the surface plasmon induced absorption enhancement due to the enhancement of local electric field near the hot spots, the other is

surface plasmon coupled emission (SPCE), which is achieved by energy transfer from fluorophores in close vicinity of metal surface to the induced surface plasmon modes and then reradiated to free space through the reverse process of surface plasmon resonance (SPR). There are very clear physical picture and direct experimental evidence for the mechanism of surface plasmon induced absorption enhancement.¹⁵ In the case of SPCE, even many works have reported on the characteristics of directional emission and high p-polarization,^{23,26,27} there are few works on further details for the comprehension of its mechanism using time-resolved techniques.²⁸

In the present work, we observe directional emission and high p-polarization of SPCE using tris(8-hydroxyquinoline)-aluminum (Alq₃) on silver gratings and show the time-resolved fluorescence anisotropy of this kind of emission at different detection angles. Our choices for fluorophores, grating period, and excitation wavelength allow us to study the phenomenon of SPCE excluding surface plasmon induced absorption enhancement effect. Our result shows that the value of time-resolved fluorescence anisotropy for SPCE keeps constant and that the experimental value is in good agreement with the calculated result. Our work presents a step toward the deep comprehension of SPCE, comparing to the previous reports based on conventional steady-state measurements.^{29–31}

Received: August 23, 2013

Revised: November 17, 2013

Published: November 27, 2013

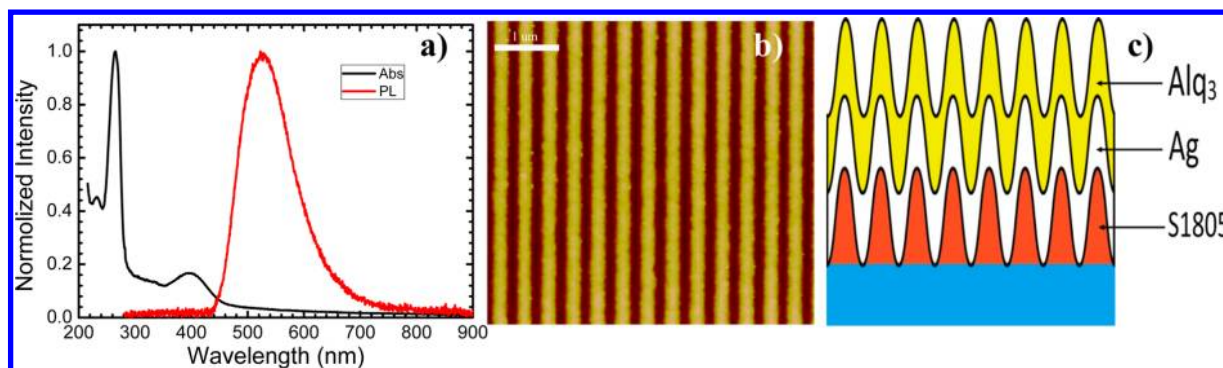


Figure 1. (a) Absorption and emission spectra of Alq₃ on plate quartz substrate; (b) AFM image of 375 nm period gratings; (c) schematic structures of the sample.

THEORY

Since the phenomenon of SPCE is considered as the reverse process of SPR,^{27,32} it can be partly understood from the physics of SPR.^{1,2} Considering the free electrons in the metal, the dielectric constant of a metal in a complex quantity is given by

$$\epsilon_m = \epsilon_r + i\epsilon_{im} \quad (1)$$

The subscripts indicate the real (r) and imaginary (im) components and *i* is the imaginary unit. We can obtain the wave-vector of SPPs according to the well-known dispersion relationship

$$k_{sp} = \left(\frac{\omega}{c}\right) \sqrt{\frac{\epsilon_r \epsilon_d}{\epsilon_r + \epsilon_d}} \quad (2)$$

k_{sp} is the in-plane wave-vector of the SPPs. ω and c are, respectively, the angular frequency and the speed of light in free space. ϵ_r and ϵ_d are the real parts of the dielectric constants of the metal and the dielectric adjacent to the metal. The wave-vector of incident light is written by

$$k_{in} = \frac{2\pi}{\lambda_{in}} = \frac{n\omega}{c} = nk_0 \quad (3)$$

where k_0 is the wave-vector of light in free space, n is the refractive index of the dielectric adjacent to the metal surface, λ_{in} is the wavelength of light in the adjacent dielectric. When the incident light hits the metal grating surface, the diffraction gives rise to a series of diffracted waves. The projection of the wave-vector for diffracted light along x -axis is

$$k_x = k_{in} \sin \theta_{in} \pm m \frac{2\pi}{\Lambda} \quad (4)$$

where θ_{in} is the incident angle, Λ is the grating period, and m is an integer. The phase-matching conditions are satisfied and the SPR absorption occurs when

$$k_x = k_{in} \sin \theta_{in} \pm m \frac{2\pi}{\Lambda} = k_{sp} \quad (5)$$

Instead of absorption of the incident light by the SPR, the phenomenon of SPCE is the emission of light through the surface plasmon modes induced by the near-field interaction between nearby excited fluorophores and the metal surface. So the wave-vector of the emitted light can be given by

$$k_{out} = \frac{k_{sp} \mp m \frac{2\pi}{\Lambda}}{\sin \theta_{out}} \quad (6)$$

where θ_{out} is the exit angle, which is the angle measured with respect to the surface normal.

Actually, SPCE and SPR occur over a relatively narrow range of angles according to the resonance response of the metal and optical constants of the adjacent dielectric. The angle-dependent absorption curves can be calculated with commercial software,²⁷ web-based software,³³ or homemade codes.⁹

EXPERIMENTAL SECTION

Sample Preparation. In our experiment, glass substrates were cleaned by the following procedure: successive sonication in deionized water, acetone, and isopropyl alcohol baths for 20 min each. After drying, the substrates were spin-coated with a thin photoresist (S1805) layer of about 120 nm thickness at 3000 rpm. The photoresist films were then exposed 150 ms with a two-beam interference microfabrication system using single-frequency 266 nm deep-ultraviolet laser and developed to form surface-relief gratings with periods of 375 nm and depth of about 50 nm. The samples were then deposited with a 50 nm thick film of silver, followed by a 30 nm thick film of tris(8-hydroxyquinoline)aluminum (Alq₃) using vacuum thermal evaporation method (evaporation rate 1 Å/s in a thermal evaporation chamber with the high vacuum of 5×10^{-4} Pa). The silver and Alq₃ layers replicated the surface profile of photoresist, producing the same period of gratings throughout the structure. The morphologies of the grating structures were characterized by an atomic force microscopy (AFM, iCON, Veeco) in tapping mode.

Steady-State Spectra Measurements. Absorption spectra measurements were performed by a Shimadzu UV-2550 spectrophotometer, and emission spectra were measured with an AvaSpec-2048 fiber optic spectrometer with 405 nm excitation beam generated from a continuous diode laser. A Glan-prism polarizer was used to polarize the excitation beam, and the polarization of the excitation beam could be changed by a half-wave plate. The sample was fixed on a rotary stage to enable excitation and collection at any desired angle. The illumination geometry of our experimental setup is provided in the Supporting Information.

Time-Resolved Fluorescence Anisotropy. Time-resolved fluorescence experiments were performed by the time-correlated single-photon counting (TCSPC) system using single-channel method. A 405 nm picosecond diode laser (Edinburgh Instruments EPL405, repetition rate 20 MHz) was used to excite the samples, and the pulses were polarized through a Glan-prism polarizer. The emitted fluorescence photons were selected by a monochromator and then collected

by a photomultiplier tube (Hamamatsu H5783p) connected to a TCSPC board (Becker and Hickel SPC-130). For our system, the time constant of the instrument response function (IRF) was about 220 ps. A polarizer was placed in front of the entrance slit of the monochromator. Using the vertically polarized excitation laser, we obtained the fluorescence decay kinetics for vertically and horizontally polarized emission, respectively.

RESULTS AND DISCUSSION

Figure 1a shows the steady-state absorption and emission spectra of AlQ_3 on plane quartz substrate. For absorption, there is one strong band peaking at 264 nm and a weak band peaking at 400 nm. In the case of emission, there is only one broad band peaking at 525 nm. There is almost no overlap region between absorption and emission bands. Figure 1b shows the AFM image of gratings with 375 nm periods, and Figure 1c is the sample structure.

Directional Emission. Lakowicz et al. had demonstrated that SPCE would occur irrespective of excitation mode.²¹ When the incident light could not induce the SPPs, SPCE could be demonstrated and studied convincingly. In our recent work, the 400 nm incident beam could only excite the AlQ_3 molecules because no angle would make the phase-matching condition become satisfied on 375 nm silver gratings (eq 5). Without the interference of surface plasmon induced absorption enhancement, SPCE could only be induced after the excitation of fluorophores through near-field interactions between fluorophores and metallic film. Our system is the optimum one to allow us to study SPCE on metal gratings, where the results were as convincing as that using the reverse Kretschmann configuration (RK).^{20,21} In our experiments, 30 nm thick AlQ_3 presented the maximum SPCE phenomenon. At the distance below 20 nm, quenching suppressed SPCE. When the AlQ_3 film was much thicker than 30 nm, the free-space radiation of fluorophores dominated the profile of emission spectra. This was consistent with the published results.²⁰

Figure 2 shows the angle-dependent emission spectra. Comparing with the original emission spectrum of AlQ_3

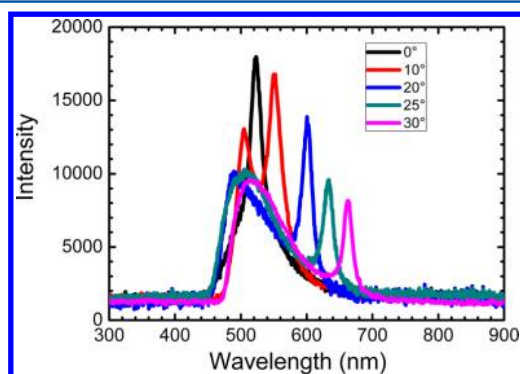


Figure 2. Emission spectra detected at different geometrical detection angles.

shown in Figure 1, the profile was reshaped at all geometrical detection angles. At 0° , the profile of the spectrum presents a sharp peak at 523 nm with full width at half-maximum (fwhm) of about 40 nm. At 10° , the peak at 523 nm is split into two peaks. One peak shifts to 504 nm, and the other one shifts to 552 nm. In the case of 20° , the blue peak shifts to about 486 nm and the red one shifts to 600 nm. Beyond 20° , the blue

peak disappears, then the natural emission spectrum of AlQ_3 is present because of the background fluorophore radiation. The red one can still be detected with considerable intensity, and the fwhm of the spectrum decreases to nearly 20 nm. The incident angle was 40° for our measurements. We had performed the experiments at different incident angles, and there was no detectable difference for the emission spectra when the incident angle changed from 0° to 40° . There was also no detectable difference for the emission spectra when we changed the polarization of the incident beam from s-polarization to p-polarization (seen in Supporting Information S6). According to the previous calculations,³⁴ at the distance of 20–30 nm in close vicinity to metal film, the fluorophores with orientation of perpendicular dipoles contributed to SPCE much more than that of parallel dipoles. In the AlQ_3 film, the fluorophores were oriented randomly. The s-polarization and p-polarization incident beams could excite the fluorophores with orientation of perpendicular dipoles at the same probability. In addition, both polarized incident beams could not induce the SPPs. So our results using s-polarization and p-polarization incident beams were reasonable.

p-Polarized Emission. The high p-polarization is a notable characteristic of SPCE.²³ Figure 3 shows the p-polarization

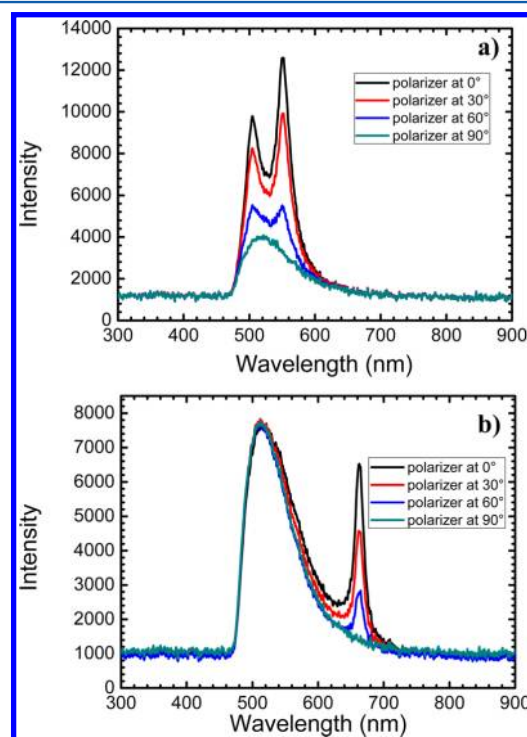


Figure 3. Polarization of the emission spectra at geometrical detection angles of 10° (a) and 30° (b), the angles of polarizer in the labels are related to the p-polarization.

characteristic of the emission peaks, which reshape the original profile of emission spectrum. We chose two representative geometrical detection angles at 10° (Figure 3a) and 30° (Figure 3b). The emission spectra detected at other angles presented the similar properties.

In Figure 3a, when we rotated the polarizer in front of the detector from p-polarization to s-polarization, the two peaks at 504 and 552 nm disappeared. The magnitude of the polarization is between 0.7 and 0.8. The remaining signal is the same with the original emission spectrum of AlQ_3 on plate

substrate (seen in Figure 1). There must be some fluorophores that do not contribute to SPCE and deactivate through the free-space radiation process. The detected spectra were the overlap of the free-space emission and SPCE. In the case of 30° (seen in Figure 3b), we can also detect the free-space emission signature, but the p-polarized emission profile peaking at 663 nm shifts to the tail of the original emission profile. Without the interference of the free-space emission background, the magnitude of the polarization for the extra emission peak is more than 0.9. This is in good agreement with the results obtained using the RK configuration.²⁷

FDTD Simulation. The absorption dispersion curves and distribution of the magnetic field intensity were simulated for our corrugated samples employing a finite difference time domain (FDTD) method using the homemade FDTD codes.⁹ The simulated absorption dispersion curves for p-polarization of our corrugated structures are shown in Figure 4a, in which

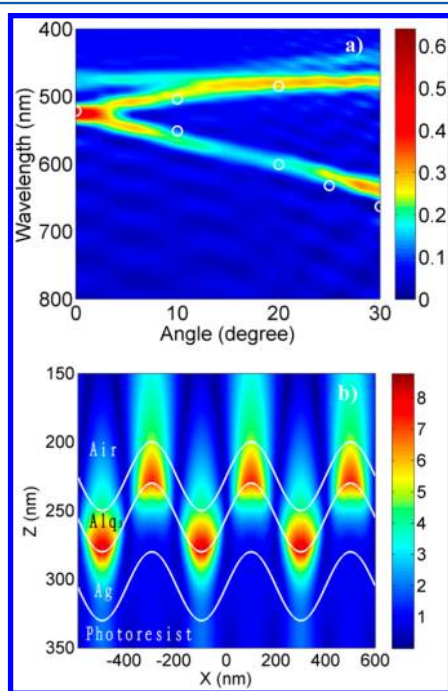


Figure 4. (a) Simulated absorption dispersion curves with experimental data (white circles); (b) the distribution of magnetic field intensity in our corrugated structures at the wavelength of 523 nm.

the absorption intensity appears as a function of both wavelengths and incident angles. The dispersion relation curves constructed from the experimental SPCE spectra are also plotted. It can be seen clearly that the experimental results are in good agreement with the numerical simulations. Figure 4b presents the field distribution in p-polarization at incident angle 0° , which correspond to the peak wavelength of 523 nm for the measured SPCE spectra. The match between the angular distribution of SPCE and the absorption dispersion relation curves appears to be attributed to a near-field interaction of the excited fluorophores with SPPs mode due to the adjacent metal film.

Fluorescence Anisotropy. The steady-state measurements and numerical simulations have demonstrated angular distribution and p-polarization of the emission reshaping the original fluorescence emission profile. Our results are consistent

with the characteristics of SPCE with the reverse Kretschmann configuration. In order to obtain the further details for SPCE, we adopted the TCSPC system to perform the time-resolved fluorescence anisotropy measurements.

Figure 5 presents the delay traces of time-resolved fluorescence anisotropy. Figure 5a,b shows the relaxation traces of fluorescence anisotropy at 504 and 552 nm at 10° , corresponding to the emission spectra shown in Figure 3a. At 504 nm, the value of the anisotropy keeps constant at about -0.1 during the whole decaying process (Figure 5a), and at 552 nm, the value of the anisotropy keeps constant at about -0.2 during the whole decaying process (Figure 5b). Figure 5c,d shows the relaxation traces of fluorescence anisotropy at 520 and 663 nm at 30° , corresponding to the emission spectra shown in Figure 3b. At 520 nm, the value of fluorescence anisotropy keeps constant at about zero, which is consistent with the anisotropy values measured using samples on plate substrate and bare grating without silver (seen in Supporting Information S2 and S3). In the case of 663 nm, the value of fluorescence anisotropy keeps constant at -0.45 . In our above discussions, the detected emission profile is a mixture of SPCE and the free-space radiation background at 10° . The time-resolved anisotropy value must be affected by the background free-space emission. In the case of 30° , SPCE would not be affected by the free-space emission for the p-polarized peak shifts to the tail of the background emission profile. So the value of -0.45 exhibits the nature of the time-resolved fluorescence anisotropy for SPCE during the relaxation process, which is close to the theoretical value -0.5 calculated by the equation³⁵

$$r(t) = \frac{I_{VV}(t) - GI_{VH}(t)}{I_{VV}(t) + 2GI_{VH}(t)} \quad (7)$$

where G is a correction factor that was used to correct the different transmission efficiency of the monochromator for vertically and horizontally polarized light. The G factor of our system had been obtained before the performance of the anisotropy measurements.

CONCLUSIONS

In summary, we fabricated Alq₃ on silver grating structures, which exhibited the reshaped emission spectra due to the mixing of the SPCE and the original emission of fluorophores. The designed parameters in our experiments allowed us to observe the angular distribution and the p-polarized characteristics of the extra emission peaks without the interference of surface plasmon induced absorption, and the FDTD simulations were in excellent agreement with the experimental data. The time-resolved fluorescence anisotropy experiments were performed, and we obtained the value of -0.45 , which could present the nature of the time-resolved fluorescence anisotropy for SPCE during the relaxation process and was a deeper understanding for the SPCE using time-resolved techniques. The unique characteristics of SPCE, such as wavelength resolution ability and enhanced fluorescence emission with highly polarization, enable it with numerous potential applications on optical switches, increasing the efficiency of OLED devices, medical diagnostics, and biological sensors.

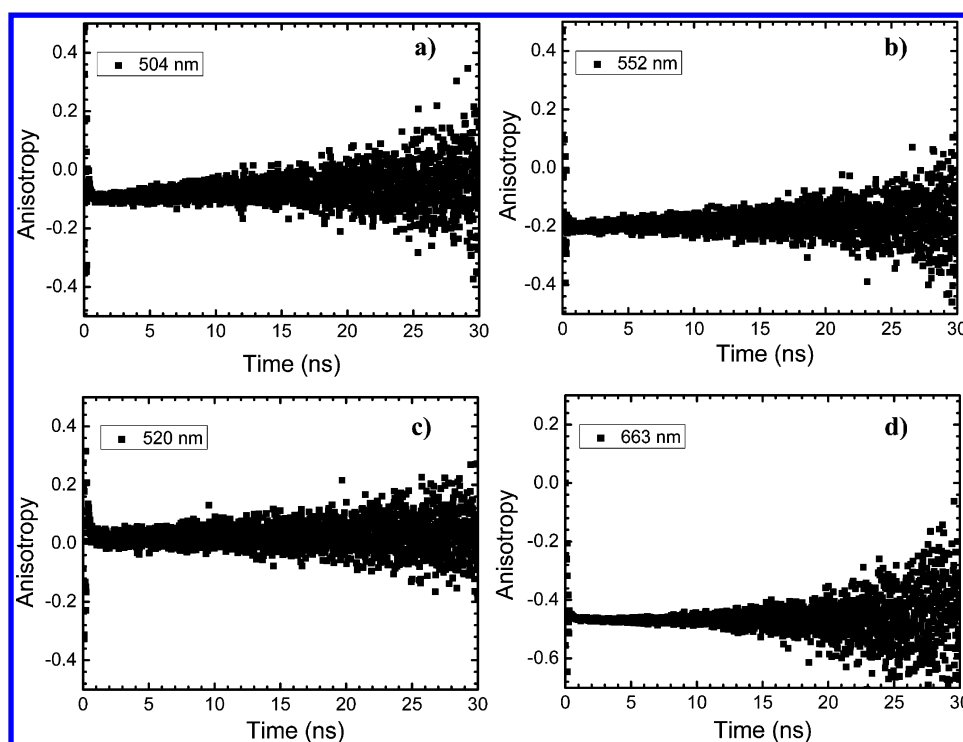


Figure 5. Time-resolved fluorescence anisotropy traces at 504 nm (a) and 552 nm (b) for the geometrical detection angle of 10° ; and at 520 nm (c) and 663 nm (d) for the geometrical detection angle of 30° .

■ ASSOCIATED CONTENT

Supporting Information

Illumination geometry of our experimental setup for directed emission; time-resolved fluorescence anisotropy traces; fluorescence decay curves; and emission spectra. This material is available free of charge via the Internet at <http://pubs.acs.org>.

■ AUTHOR INFORMATION

Corresponding Authors

*(H.-Y.W.) E-mail: haiyu_wang@jlu.edu.cn.

*(H.-B.S.) E-mail: hbsun@jlu.edu.cn.

Notes

The authors declare no competing financial interest.

■ ACKNOWLEDGMENTS

We would like to acknowledge Natural Science Foundation China (NSFC) under Grant no. 21273096 and Doctoral Fund of Ministry of Education of China under Grant no. 20130061110048 for support.

■ REFERENCES

- (1) Maier, S. A. *Plasmonics: Fundamentals and Applications*; Springer: New York, 2007.
- (2) Brongersma, M. L.; Kik, P. G. *Surface Plasmon Nanophotonics*; Springer: Dordrecht, Netherlands, 2007.
- (3) Homola, J. *Surface Plasmon Resonance Based Sensors*; Springer: Berlin, Germany, 2006.
- (4) Atwater, H. A.; Polman, A. Plasmonics for Improved Photovoltaic Devices. *Nat. Mater.* **2010**, *9*, 205–213.
- (5) Nishijima, Y.; Ueno, K.; Yokota, Y.; Murakoshi, K.; Misawa, H. Plasmon-Assisted Photocurrent Generation from Visible to Near-Infrared Wavelength Using a Au-Nanorods/TiO₂ Electrode. *J. Phys. Chem. Lett.* **2010**, *1*, 2031–2036.
- (6) Jin, Y.; Feng, J.; Zhang, X. L.; Xu, M.; Bi, Y. G.; Chen, Q. D.; Wang, H. Y.; Sun, H. B. Surface-Plasmon Enhanced Absorption in

Organic Solar Cells by Employing a Periodically Corrugated Metallic Electrode. *Appl. Phys. Lett.* **2012**, *101*, 163303.

(7) Su, Y. H.; Ke, Y. F.; Cai, S. L.; Yao, Q. Y. Surface Plasmon Resonance of Layer-by-Layer Gold Nanoparticles Induced Photoelectric Current in Environmentally-Friendly Plasmon-Sensitized Solar Cell. *Light Sci. Appl.* **2012**, *1*, e14.

(8) Hobson, P. A.; Wedge, S.; Wasey, J. A. E.; Sage, I.; Barnes, W. L. Surface Plasmon Mediated Emission from Organic Light-Emitting Diodes. *Adv. Mater.* **2002**, *14*, 1393–1396.

(9) Jin, Y.; Feng, J.; Zhang, X. L.; Bi, Y. G.; Bai, Y.; Chen, L.; Lan, T.; Liu, Y. F.; Chen, Q. D.; Sun, H. B. Solving Efficiency–Stability Tradeoff in Top-Emitting Organic Light-Emitting Devices by Employing Periodically Corrugated Metallic Cathode. *Adv. Mater.* **2012**, *24*, 1187–1191.

(10) Bi, Y. G.; Feng, J.; Li, Y. F.; Jin, Y.; Liu, Y. F.; Chen, Q. D.; Sun, H. B. Enhanced Efficiency of Organic Light-Emitting Devices with Metallic Electrodes by Integrating Periodically Corrugated Structure. *Appl. Phys. Lett.* **2012**, *100*, 053304.

(11) Yokota, Y.; Ueno, K.; Misawa, H. Highly Controlled Surface-Enhanced Raman Scattering Chips Using Nanoengineered Gold Blocks. *Small* **2011**, *7*, 252–258.

(12) Rycenga, M.; Cobley, C. M.; Zeng, J.; Li, W.; Moran, C. H.; Zhang, Q.; Qin, D.; Xia, Y. Controlling the Synthesis and Assembly of Silver Nanostructures for Plasmonic Applications. *Chem. Rev.* **2011**, *111*, 3669–3712.

(13) Verma, P.; Ichimura, T.; Yano, T.-A.; Saito, Y.; Kawata, S. Nano-Imaging Through Tip-Enhanced Raman Spectroscopy: Stepping Beyond the Classical Limits. *Laser Photonics Rev.* **2010**, *4*, 548–561.

(14) Lozano, G.; Louwers, D. J.; Rodriguez, S. R.; Murai, S.; Jansen, O. T.; Verschuuren, M. A.; Rivas, J. G. Plasmonics for Solid-State Lighting: Enhanced Excitation and Directional Emission of Highly Efficient Light Sources. *Light Sci. Appl.* **2013**, *2*, e66.

(15) Jiang, Y.; Wang, H. Y.; Wang, H.; Gao, B. R.; Hao, Y. W.; Jin, Y.; Chen, Q. D.; Sun, H. B. Surface Plasmon Enhanced Fluorescence of Dye Molecules on Metal Grating Films. *J. Phys. Chem. C* **2011**, *115*, 12636–12642.

- (16) Rivas, J. G.; Vecchi, G.; Giannini, V. Surface Plasmon Polariton-Mediated Enhancement of the Emission of Dye Molecules on Metallic Gratings. *New J. Phys.* **2008**, *10*, 105007.
- (17) Knoll, W.; Philpott, M. R.; Swalen, J. D.; Girlando, A. Emission of Light from Ag Metal Gratings Coated with Dye Monolayer Assemblies. *J. Chem. Phys.* **1981**, *75*, 4795–4799.
- (18) Cui, X.; Tawa, K.; Hori, H.; Nishii, J. Duty Ratio-Dependent Fluorescence Enhancement Through Surface Plasmon Resonance in Ag-Coated Gratings. *Appl. Phys. Lett.* **2009**, *95*, 133117.
- (19) Hung, Y. J.; Smolyaninov, I. I.; Davis, C. C.; Wu, H. C. Fluorescence Enhancement by Surface Gratings. *Opt. Express* **2006**, *14*, 10825–10830.
- (20) Lakowicz, J. R. Radiative Decay Engineering 3. Surface Plasmon-Coupled Directional Emission. *Anal. Biochem.* **2004**, *324*, 153–169.
- (21) Gryczynski, I.; Malicka, J.; Gryczynski, Z.; Lakowicz, J. R. Radiative Decay Engineering 4. Experimental Studies of Surface Plasmon-Coupled Directional Emission. *Anal. Biochem.* **2004**, *324*, 170–182.
- (22) Lakowicz, J. R. Radiative Decay Engineering 5: Metal-Enhanced Fluorescence and Plasmon Emission. *Anal. Biochem.* **2005**, *337*, 171–194.
- (23) Cao, S. H.; Cai, W. P.; Liu, Q.; Li, Y. Q. Surface Plasmon-Coupled Emission: What Can Directional Fluorescence Bring to the Analytical Sciences? *Annu. Rev. Anal. Chem.* **2012**, *5*, 317–336.
- (24) Enderlein, J.; Ruckstuhl, T. The Efficiency of Surface-Plasmon Coupled Emission for Sensitive Fluorescence Detection. *Opt. Express* **2005**, *13*, 8855–8865.
- (25) Fort, E.; Gresillon, S. Surface Enhanced Fluorescence. *J. Phys. D: Appl. Phys.* **2008**, *41*, 013001.
- (26) Gryczynski, I.; Malicka, J.; Jiang, W.; Fischer, H.; Chan, W. C. W.; Gryczynski, Z.; Grudzinski, W.; Lakowicz, J. R. Surface-Plasmon-Coupled Emission of Quantum Dots. *J. Phys. Chem. B* **2005**, *109*, 1088–1093.
- (27) Gryczynski, I.; Malicka, J.; Gryczynski, Z.; Lakowicz, J. R. Surface Plasmon-Coupled Emission with Gold Films. *J. Phys. Chem. B* **2004**, *108*, 12568–12574.
- (28) Wang, Y.; Yang, T.; Pourmand, M.; Miller, J. J.; Tuominen, M. T.; Achermann, M. Time-Resolved Surface Plasmon Polariton Coupled Exciton and Biexciton Emission. *Opt. Express* **2010**, *18*, 15560–15568.
- (29) Sullivan, K. G.; King, O.; Sigg, C.; Hall, D. G. Directional, Enhanced Fluorescence from Molecules Near a Periodic Surface. *Appl. Opt.* **1994**, *33*, 2447–2454.
- (30) Tawa, K.; Hori, H.; Kintaka, K.; Kiyosue, K.; Tatsu, Y.; Nishii, J. Optical Microscopic Observation of Fluorescence Enhanced by Grating-Coupled Surface Plasmon Resonance. *Opt. Express* **2008**, *16*, 9781–9790.
- (31) Geiger, C.; Fick, J. Surface Plasmon-Mediated Far-Field Emission of Laser Dye Solutions. *Opt. Lett.* **2010**, *35*, 2245–2247.
- (32) Noginov, M. A.; Zhu, G.; Mayy, M.; Ritzo, B. A.; Noginova, N.; Podolskiy, V. A. Stimulated Emission of Surface Plasmon Polaritons. *Phys. Rev. Lett.* **2008**, *101*, 226806.
- (33) Nelson, B. P.; Frutos, A. G.; Brockman, J. M.; Corn, R. M. Near-Infrared Surface Plasmon Resonance Measurements of Ultrathin Films. I. Angle Shift and SPR Imaging Experiments. *Anal. Chem.* **1999**, *71*, 3928–3934.
- (34) Ford, G. W.; Weber, W. B. *Electromagnetic Interactions of Molecules with Metal Surfaces*; North-Holland Physics Publishing: Amsterdam, Netherlands, 1984; Vol. 113.
- (35) Lakowicz, J. R. *Principles of Fluorescence Spectroscopy*; Springer: New York, 2006.